Jurnal Teknologi, 47(D) Dis. 2007: 103–120

DESIGN, MODELING, AND PERFORMANCE COMPARISON OF FEEDING TECHNIQUES FOR A MICROSTRIP PATCH ANTENNA

P. J. SOH[1], M. K. A. RAHIM[2], A. ASROKIN[3] & M. Z. A. ABDUL AZIZ[4]

Abstract. Microstrip patch antennas has a variety of feeding technique applicable to them. It can be categorized in accordance to the main power transfer mechanism from the feed line to the patch. Contacting feeds investigated in this work are coaxial probe feed and transmission line feed; while non-contacting feeds which are proximity-coupled-fed and the aperture-coupled-fed. This work is an effort to design, model, simulate, fabricate and measure all four different types of microstrip antenna's of non-contacting feed and contacting feed techniques on a similar sized, rectangular patch. Simulation is done using the circuit model (CM) derived from the Transmission Line Model (TLM), and is compared with another simulation set of feeding methods produced using the Method of Moments (MoM). Both methods are simulated on Microwave Office. This design intends to focus on studying the differences in measured and simulated parameters of the patch and its respective feeds, simulate it using MoM, and finally, the fabrication process. Radiation measurements are also presented. Designs for each feeding technique achieved the best return loss (RL) at the desired frequency range of 2.4 GHz. The fabricated hardware produced good RL, bandwidth (BW), and comparable radiation performance compared against simulation using MoM. All antennas produced maximum E-and H-plane co- and cross-polarization difference in the magnitude of -18 dB and half-power beam widths (HPBW) in the magnitude of 90^{o}.

Keywords: Circuit modeling, microstrip antennas, coaxial probe feed, transmission line feed, proximity coupled feed, aperture coupled feed

Abstrak. Antena mikrojalur tampal mempunyai pelbagai teknik suapan terhadapnya. Teknik ini boleh dikategorikan kepada mekanisma untuk pemindahan kuasa maksimum daripada talian suapan kepada antena tampal. Suapan secara langsung yang dijalankan dalam kerja ini terdiri daripada suapan prob sepaksi dan suapan talian penghantaran manakala suapan tak secara langsung adalah suapan jenis proximiti dan suapan bukaan. Kerja ini adalah usaha untuk mereka bentuk, model, simulasi dan pengukuran untuk keempat jenis suapan antena mikrojalur pada saiz yang sama bagi antena tampal segi empat tepat. Simulasi dilakukan menggunakan model litar yang dihasilkan daripada model talian penghantaran dan dibandingkan dengan simulasi menggunakan cara momen (MoM) dan akhirnya proses fabrikasi. Pengukuran sinaran juga dipersembahkan. Reka bentuk untuk setiap teknik suapan di capai dengan nilai kehilangan balikan pada frekuensi yang dikehendaki, iaitu 2.4 GHz. Fabrikasi

[1,2&3] Wireless Communication Center (WCC), Electrical Engineering Faculty, Universiti Teknologi Malaysia, 81310 Skudai, Johor, Malaysia.
Email: sohpingjack@gmail.com, mkamal@fke.utm.my, awi1982@yahoo.com

[4] Dept of Telecommunication Electronics, Universiti Teknikal Malaysia Melaka (UTeM), Locked Bag 1200, Ayer Keroh, 75450 Melaka, Malaysia.
Email: mohamadzoinol@utem.edu.my

kakasan menghasilkan kehilangan balikan yang baik, lebar jalur dan prsetasi sinaran yang agak baik dibandingkan dengan simulasi menggunakan MoM. Kesemua antena menghasilkan satah E dan H yang maksimum dan pengutuban silang sebanyak -18 dB dan lebar alur separuh kuasa pada magnitud 90°.

Kata kunci: Pemodelan litar, antena mikrojalur, suapan prob sepaksi, suapan talian penghantaran, suapan proximiti , suapan bukaan

1.0 INTRODUCTION

Microstrip patch antennas (MPAs) have several well-known feeding techniques, which are coaxial probe feed (CPF), microstrip transmission line feed (TLF), proximity coupled feed (PCF) and aperture coupled feed (ACF). Direct contacting feeds such as CPF and TLF; as its name implies, transfer the power fed into the MPA directly via a conducting feed line connected to the patch conductor [1]. In non-contacting feeds, the laminates are separated by a ground plane and coupling between the microstrip feed line, and the patch antenna is achieved either electromagnetically or via a small slot on the ground plane. No vertical interconnects are required for these feeds, simplifying the fabrication processes and also adhering to the conformal nature of printed circuit technology.

2.0 ANTENNA AND FEED DESIGN

To ensure a fair comparison between the techniques, all feeds are designed to feed a rectangular-shaped microstrip patch antenna. The antenna is designed to resonate at the frequency of 2.4 GHz. A suitable and similar substrate and simulation tool is also chosen to ensure uniformity with least alteration to the feeds' original structure. The substrate used is FR-4, which has a dielectric constant (ε_r) of 4.5, dielectric loss tangent ($tan\ \delta$) of 0.019 and a single layered substrate height (h) of 1.6 mm. Verification of the comparisons are done by generating two sets of simulation results. A similar simulation software (Microwave Office) is used, but different models are simulated in different simulation environments. One uses the Method of Moments (MoM) while the other applies the Circuit Model/Schematic (CM), which is derived from the Transmission Line Matrix (TLM). Both differ in terms of numerical assumptions at derivation level, which causes different amount of simulation resources' utilization, at the expense of accuracy. In other words, TLM will cost least time and simulation resources, but it will produce a less accurate results, while MoM will produce more accurate results but at the same time take up more resources. Fabrication of the device is done using the wet-etch technique on a FR-4 photo board, which layouts are similar to MoM based simulations. Device measurement values are collected, compared and analyzed against the simulation results.

In order to design a patch resonating at a similar frequency of 2.4 GHz, the equations in Table 1 are used. However, a significant upwards shift in resonant frequency (f_{res})

Table 1 The design equations for different parameters in designing an MPA

Step	Parameter	Design equation	Legend
1	Patch Width (W)	$W = \frac{1}{2f\left(\sqrt{\varepsilon_o \mu_o}\right)}\sqrt{\frac{2}{\varepsilon_r + 1}}$	ε_{reff} = effective dielectric constant h = substrate height
2	Effective Dielectric Constant (ε_{reff})	$\varepsilon_{reff} = \left(\frac{\varepsilon_r + 1}{2}\right) + \left[\left(\frac{\varepsilon_r - 1}{2}\right)\left[1 + 12\frac{h}{W}\right]^{-0.5}\right]$	W = patch width ε_r = relative dielectric constant μ_o = permeability in free space
3	Patch Length Extension (ΔL)	$\Delta L = 0.412h\frac{\left(\varepsilon_{reff} + 0.3\right)\left(\frac{W}{h} + 0.264\right)}{\left(\varepsilon_{reff} - 0.258\right)\left(\frac{W}{h} + 0.8\right)}$	Le = relative dielectric constant ΔL = patch length extension
4	Patch Length (L)	$L = \left(\frac{1}{2f\sqrt{\varepsilon_{reff}}\sqrt{\varepsilon_o \mu_o}}\right) - 2\Delta L$	
5	Effective Patch Length (L_e)	$Le = L + 2\Delta L$	

has been reported due to the coupling between the antenna and the transmission line [2]. Therefore before designing the patch, a lower design frequency is necessary. The shift values have been determined experimentally to compensate for the amount of upward shifts. A prototype with different feeds has been fabricated and also its amount of shift has been calculated so that it could be taken into consideration when designing for the actual prototypes. The results are shown in Table 2 and Table 3. Calculated values are approximate values of the resonant parameters, but minor tweaking to the values provided by the software is necessary to achieve optimal simulation results at desired resonance.

Table 2 Amount of resonant frequency shift determined by simulation and experimentally

Type of feed	Rep model	Return loss (dB)	Resonant freq (GHz)	Freq shift (%)	New design freq (GHz)
Coaxial	MoM	–30.16	2.45	4.583	2.29
Probe Feed	Meas	–15.17	2.56		
Microstrip	MoM	–25.33	2.41	2.075	2.36
Line Feed	Meas	–17.63	2.48		
Aperture	MoM	–21.093	2.30	2.128	2.35
Coupled Feed	Meas	–14.98	2.35		
Proximity	MoM	–26.57	2.38	2.917	2.33
Coupled Feed	Meas	–13.87	2.45		

Table 3 New resonant frequency determined experimentally

Type of feed	Rep model	Resonant freq (GHz)	Freq shift (%)	New design freq (GHz)	Calculated at new freq *W* (mm)	Calculated at new freq *L* (mm)	Actual *W* (mm)	Actual *L* (mm)
Coaxial Probe Feed	MoM	2.45	4.583	2.29	38.302	29.600	37.000	30.000
	Meas	2.56						
Microstrip Line Feed	MoM	2.41	2.075	2.36	39.473	30.522	39.000	29.000
	Meas	2.48						
Aperture Couple Feed	MoM	2.30	2.128	2.35	38.465	29.728	37.000	29.000
	Meas	2.35						
Proximity Coupled Feed	MoM	2.38	2.917	2.33	38.795	29.988	37.500	28.500
	Meas	2.45						

3.0 FEED MODELS & ARCHITECTURE

3.1 Coaxial Probe Feed (CPF)

A coaxial probe fed microstrip patch antenna (CPF-MPA) is fed using a coaxial probe which outer conductor is connected to the bottom ground plane. Its inner conductor extends further upwards through the substrate to connect to the patch. The structure of this feeding technique is shown in Figure 1, and its equivalent circuit in Figure 2. Impedance control is done using the probe position. Probe feed mechanism is in direct contact with the antenna, and most of the feed network is isolated from the patch. This provides an efficient feeding and minimizes spurious radiation [2]. Connection of the different inner and outer conductors to the different layers of patch, and the existence of a vertical interconnection complicates fabrication of this antenna type. It also produces small bandwidth (BW), and might generate high cross-polarized

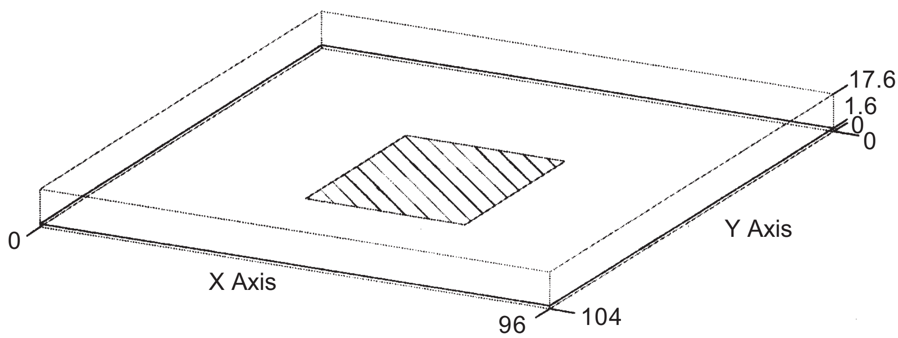

Figure 1 The 3D structure of the coaxial probe fed microstrip patch antenna

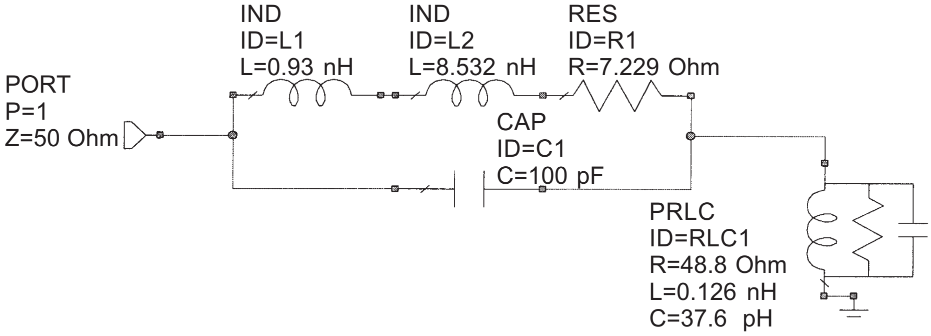

Figure 2 The equivalent circuit for coaxial probe fed microstrip patch antenna

fields when electrically thick substrates are used [3]. The parallel RLC circuit in Figure 2 represents the matched resonating patch, which is about 50Ω in complex value. Feed reactance is a combination of the inductive feed and the capacitive feed reactance between the patch and the ground. The coaxial probe is matched to the patch using three components (two inductors, *L1* and *L2*, and a resistor, *R1* in series), while the parallel capacitor value represents the probe's capacitance. For MoM simulation, the design dimensions are shown in Figure 3.

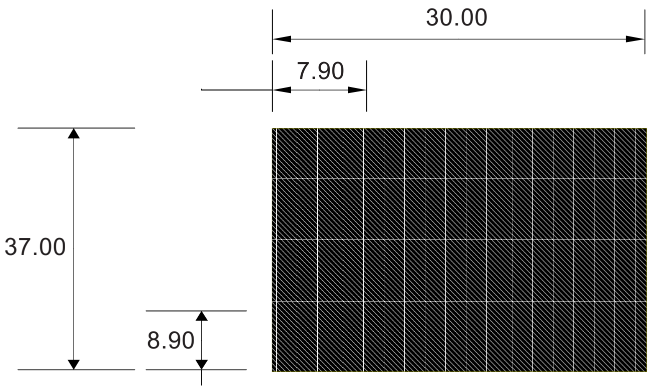

Figure 3 Dimension of the coaxial probe fed antenna

3.2 Microstrip Transmission Line Feed (TLF)

A microstrip transmission line-fed patch antenna (TLF-MPA) is generally made up feed line of a certain width and length (W_f and L_f), and connected to a specific matching stub of corresponding width and length (W_s and L_s). Its structure is shown in Figure 4. The existence of the stub is critical to match the high value of antenna's characteristic impedance to the 50Ω SMA connector, especially when it is fed along one of the radiating edges of the patch.

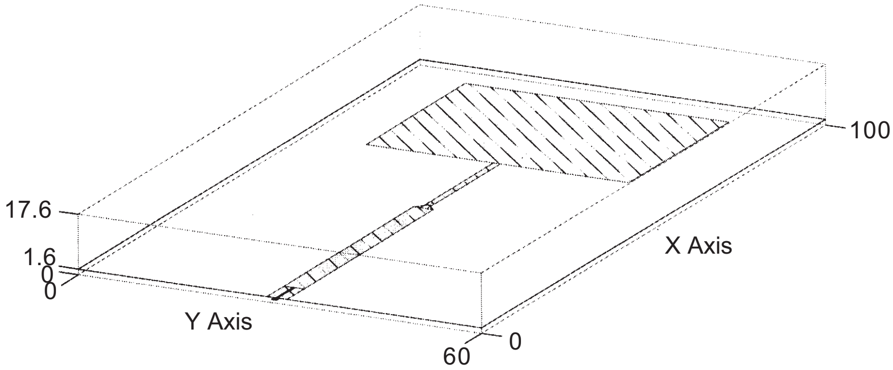

Figure 4 The 3D structure of the microstrip transmission line fed patch antenna

The feed position at the edge provides the impedance control. Since the feed and patch can be laid out and etched on one board, it eases the fabrication. The level of the input impedance is easily controlled using the matching stub. However, TLF-MPA has relatively narrow BW and gain characteristics. This technique also suffers from poor surface wave efficiency, feed network radiation and relatively high spurious feed radiation [4].

The TLF equivalent circuit used in this work is derived from [5], and is shown in Figure 5. The patch, its fringing fields, feed line; matching stub and feed-to-stub transition are all represented as microstrip lines of the equivalent calculated lengths and widths. The serial RC circuit at the edges, which also represents the fringing fields, has been calculated to have quite similar resistance and capacitance values. The dimension for the optimized feed and antenna is shown in Figure 6. The patch dimension is also listed in Table 2.

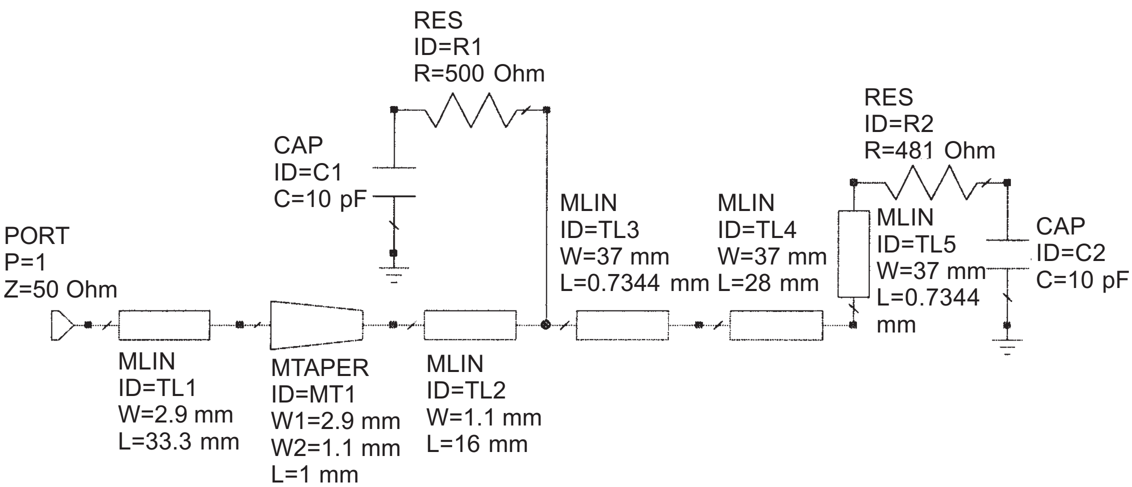

Figure 5 The equivalent circuit of the microstrip transmission line fed patch antenna

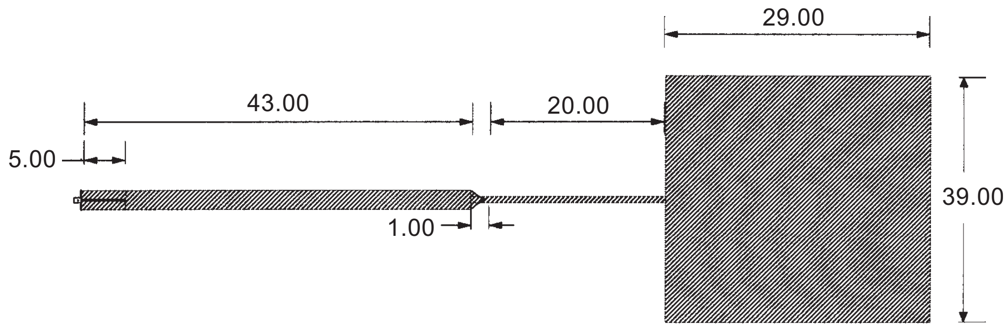

Figure 6 Dimension for the transmission line fed antenna

3.3 Proximity-Coupled Feed (PCF)

The proximity coupled fed microstrip patch antenna (PCF-MPA) consists of two layers on top of each other. A grounded substrate at the bottom layer consists of a microstrip feed line. Above this material is another dielectric layer with a patch etched on its top surface. Power from the feed network is coupled in between layers, up to the patch electromagnetically.

The structure of a PCF-MPA is shown in Figure 7. In contrast to the direct contact methods, which are predominantly inductive, the proximity-coupled patch's coupling mechanism is capacitive in nature [1]. The difference in coupling significantly affects the obtainable impedance BW, thus, BW of a PCF-MPA is inherently greater than the direct contact feed patches [6].

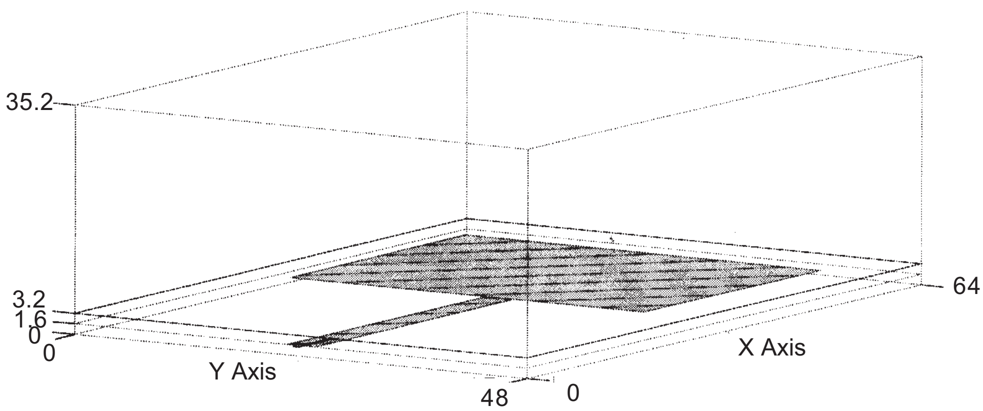

Figure 7 The 3D structure of the proximity coupled fed microstrip patch antenna

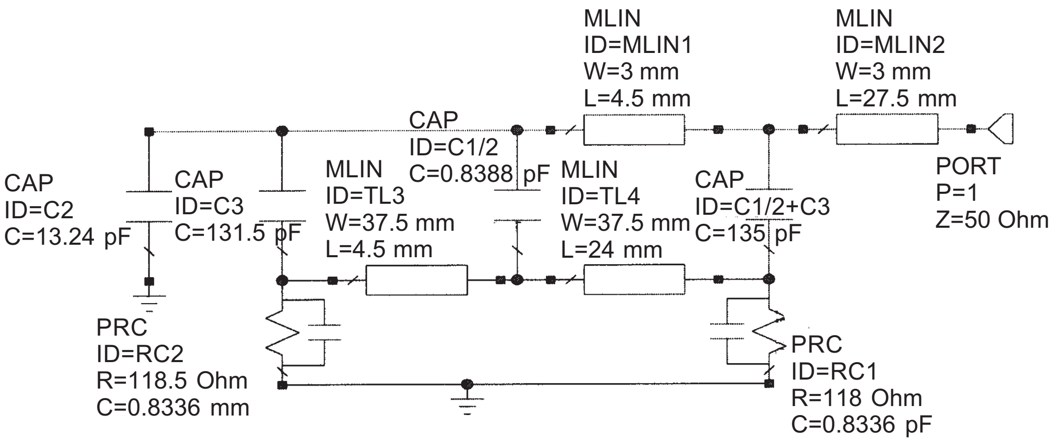

Figure 8 The equivalent circuit of the proximity coupled fed microstrip patch antenna

The CM for this feed technique is shown in Figure 8. The feed and patch are also represented by microstrip transmission lines. However, the feed line is divided into two sections, in which a section is buried underneath the patch, while the other is not. The patch section which has an overlapping feed line underneath is also segregated from the other part which has no line at the bottom. The width and length of each section are determined according to the MoM simulated dimensions. The electromagnetic coupling between patch and feed line is represented by capacitors, and this area yields the highest capacitance due to the strong coupling that exists in between. The parallel RC circuit in this model represents the dominant fringing fields that exist at the edge of the microstrip patch [7]. The resistance and capacitance values calculated in this representation are almost similar at both sides. The optimized dimension of this antenna is also listed in Table 2, and its layout is shown in Figure 9.

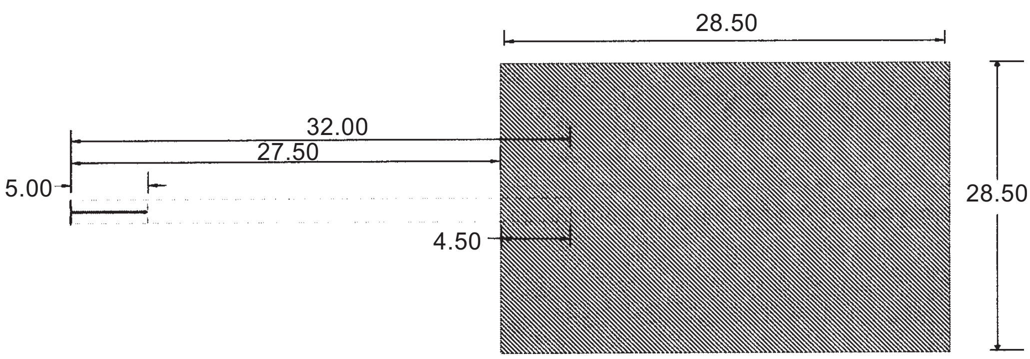

Figure 9 Dimension for the proximity coupled line fed antenna

3.4 Aperture-Coupled Feed (ACF)

In an aperture coupled-fed microstrip patch antenna (ACF-MPA), separate dielectric laminates are used for the feed network and the patch antenna, as it is in PCF-MPA. The main difference is both laminates are separated by a ground plane which consists of a coupling aperture/slot between the feed and patch antenna. The structure of this antenna is shown in Figure 10. Since all layers adhere to conformal printed circuit technology, fabrication is thus made simple. However, alignment between layers and correct selection of aperture size and position will be critical in controlling the antenna's impedance [8]. The natural existence of small gaps in between the layers of dielectric laminates can significantly alter the input impedance values. While solving this problem using conformal adhesives, the dielectric properties of the used chemical will also affect the anticipated performance [9]. Even though ACF-MPAs have almost similar BW and gain responses as the direct fed patches, this feed technique is more popular as it is very easy to significantly enhance the impedance BW of this antenna [1]. The absence of abrupt current discontinuities in ACF also makes it relatively easy to accurately model.

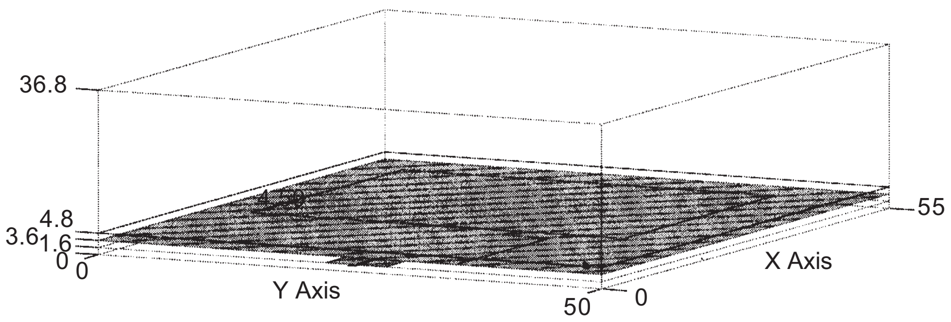

Figure 10 The 3D structure of the aperture coupled fed microstrip patch antenna

The ACF-MPA equivalent CM is presented in Figure 11. It consists of three main sections, according to its three layer structure, which are the feed section (bottom), aperture (middle) and patch (top) [10]. The length of the feed section is then subdivided into two parts, according to its position before and after the aperture slot when seen from the top. On the other hand, transmission lines representing the aperture slot are simply divided equally according to its length. The lines representing the patch are also divided according to the amount of length that it overlaps with the feed line underneath it. Instead of representing the electromagnetic coupling between the layers as capacitance, the couplings in this model are represented as transformers with the same amount of turns on each side. Despite that, fringing fields on each side of the patch are still represented using a parallel RC circuit, which capacitance and resistance

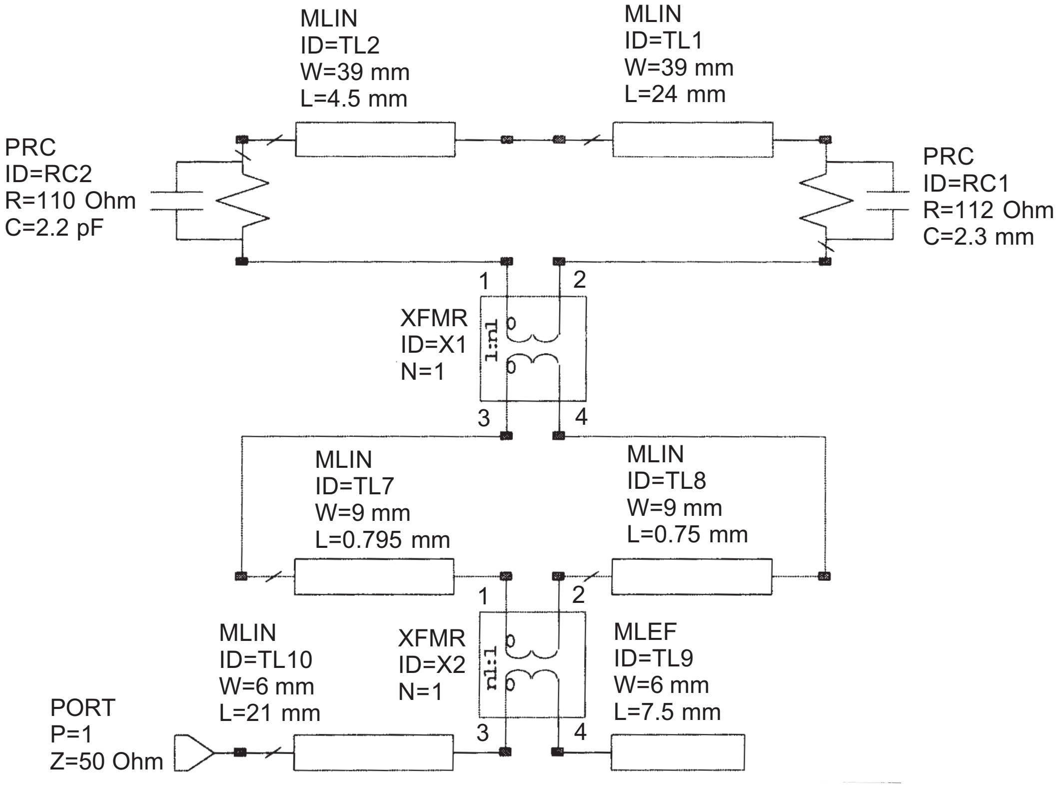

Figure 11 The equivalent circuit for an aperture coupled fed microstrip patch antenna

values are similar on both sides. The full dimension for this feed technique is shown in Figure 12.

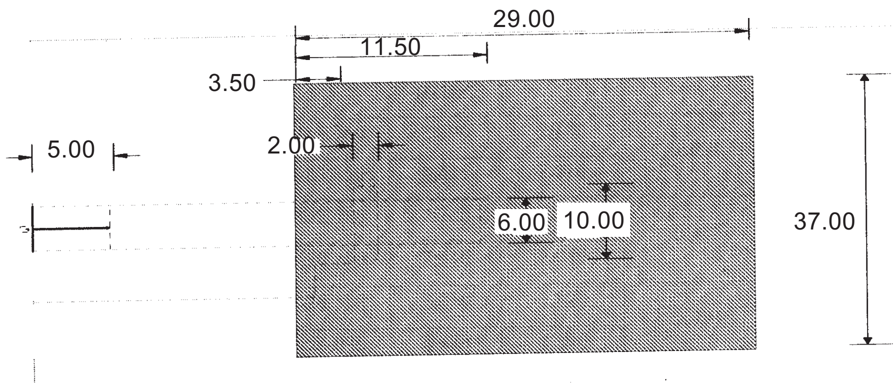

Figure 12 Dimension for the aperture coupled fed antenna

4.0 RESULTS AND DISCUSSION

4.1 MoM Simulated and Circuit Simulated Comparison

The summary of all simulated RL and BW are compiled in Table 4. It can be seen that most CMs has a large BW deviation in comparison with its MoM simulation results. Although this could reflect serious modeling defect, it also is contributed by the properties of the CM itself. In fact, CMs derived from TLM has the incapability of modeling couplings [1, 7]. This can be seen in the large BW deviation in the non-contacting feeds (PCF and ACF-MPAs), where coupling is the main mechanism of power transfer. Coupling of the antenna to the environment, which also failed to be included in CMs has also contributed to the deviations [11].

The largest BW difference between MoM and CM is produced by the CPF-MPA, up to 16%, which shows that proper improvement is needed for the model, especially in modeling the through hole and SMA connector at the bottom of patch. The TLF-MPA, on the other hand, has been represented by a very accurate model. This feed deviates less than 1% in terms of BW when CM is compared against MoM. The circuit has been made up of microstrip lines which also ease the understanding when compared to the physical layout structure [7]. Dimensions of the lines can easily be changed. Instead of representing the fringing fields as the conventional parallel RLC line, the circuit is accurately defined using the series RC element.

Despite all the large differences in BW, the CM and MoM simulated results for each feed produced rather similar RLs. However, RL differences between MoM and CM are more evident in non-contacting feeds (PCF-MPA and ACF-MPA). Since all feeds managed to produce a good RL ($<$ -10 dB), the differences will not be as critical as it is for the BW [12].

The highest f_{res} deviation produced by the PCF-MPA equivalent circuit (approximately 4% in difference) followed by the ACF-MPA, (approximately 3%) clearly proves the inability of the CMs to model couplings, since direct contact feeds such as CPF-MPA and TLF-MPA have deviations of less than 1%. Thus CMs can be used effectively when a direct contact feed is used, as it provides a more accurate result of the f_{res}.

Another possible contributor to the f_{res} differences between the MoM and CM results is due to the accuracy of the dimensions used. CMs that utilize transmission lines can be easily defined for its dimension, and a value of up to four decimal points can be used to define a certain part of its width and length. In contrast, the MoM simulated circuit has a practical capability of up to 0.1 mm resolution per simulation mesh of the enclosure. Lower sized mesh would be impractical, and would cost more in terms of simulation time and resources [3, 12].

4.2 MoM Simulated and Measurement Result Comparison

The comparison of the results in terms of BW and RL between the simulated and the measured is summarized in Table 5. The RLs generated by all feeds, which are all in the magnitudes of less than –20 dB, shows that a good impedance matching has been achieved in both designs. The best RL is shown by the TLF-MPA, while the worst RL is reflected in the PCF-MPA. This proves that the direct contact feeds easily matched as less coupling mechanism is involved. The coupling mechanism in non-contacting feeds is more critical and serves as the main mechanism of operation. It is easily affected by external elements, especially when working in a practical environment [3].

The different BW ranges produced by different MPAs are within range, as per stated in various literatures. The TLF-MPA produced the lowest measured result, and at the same time also produced the highest deviation from its simulated BW. This is caused by the feed line, which suffers serious spurious radiation in practice [2, 6]. The rest of the MPAs generated a difference of less than 6.5% between MoM and measurement since none of the feeding technique has an exposed line like the transmission line fed antenna does. Buried lines in non-contacting feeds help to minimize spurious radiation.

Table 4 MoM and circuit simulated RL, f_{res} and BW

Type of feed	Rep model	Return loss (dB)	Resonant freq (GHz)	Bandwidth (%)	Res freq variation (%)	Bandwidth variation (%)
Coaxial	MoM	–31.760	2.290	2.180	0.866	16.154
Probe Feed	Circuit	–32.660	2.310	2.600		
Microstrip	MoM	–22.480	2.360	2.540	0.840	0.787
Line Feed	Circuit	–23.619	2.380	2.520		
Aperture	MoM	–25.530	2.350	3.820	3.404	7.853
Coupled Feed	Circuit	–20.900	2.270	3.520		
Proximity	MoM	–31.934	2.320	3.840	4.132	13.75
Coupled Feed	Circuit	–28.740	2.420	3.312		

During the design stage, the hardware's upward f_{res} shift has already been compensated for. However, there still exist a small amount of f_{res} shifting from the intended design frequency of 2.4 GHz in the final measurement values. The largest amount of shift is produced by ACF-MPA which produced a f_{res} of 2.474 GHz, a shift of about 3% from 2.4 GHz. The lowest frequency shift from 2.4 GHz is shown by the transmission line feed. The fabricated hardware resonates at a frequency of 2.41 GHz, which is only less than 0.5 % in difference. The reoccurrence of the shifts are caused by several factors. First, the dielectric material used in this work, which is the FR-4 has a relative dielectric constant that varies from 4.0 to 4.8 [13], depending on the operation frequency. Unlike the constant dielectric constant defined in simulations, the material has also a varying ε_r value along the width, height and length of the structure in practice [3, 7, 11, 12]. This will also contribute to the unexpected shift in f_{res}, and better hardware measurements results could be produced when compared to simulation. Etching accuracy is also another factor to be considered; as a small change in patch's or feed's length could shift the f_{res} up to a certain amount, especially when operating in a high frequency like this. The type of chemical used, surface finish and metallization thickness are other factors that could affect the etching accuracy [3, 7, 11, 12].

4.3 Simulated and Measured Radiation Characteristics

All fabricated antennas produced satisfactory values on both E and H plane (HPBW > 20 dB). It also shows large isolations and half-power beam width (HPBW) on both E and H planes. The measurement of radiation patterns is done in anechoic chamber for all the antennas. The radiation patterns are shown in Figure 13-16, while numerical results are listed in Table 6. Since a broader E plane HPBW is produced by a smaller substrate thickness (h) [3] the largest expected E plane HPBW must be either one of the single-layered MPAs. This is proven true when CPF-MPA showed broadest HPBW pattern in E Plane, followed by TLF-MPA since both have the same values of h. The H plane HPBW grows inversely proportionate with larger W. Due to reason, the ACF-MPA again to have the largest H plane HPBW, since its patch has the largest value of W. CPF-MPA also produced a slightly lower, but almost equivalent value since it has a W value similar to CPF-MPA.

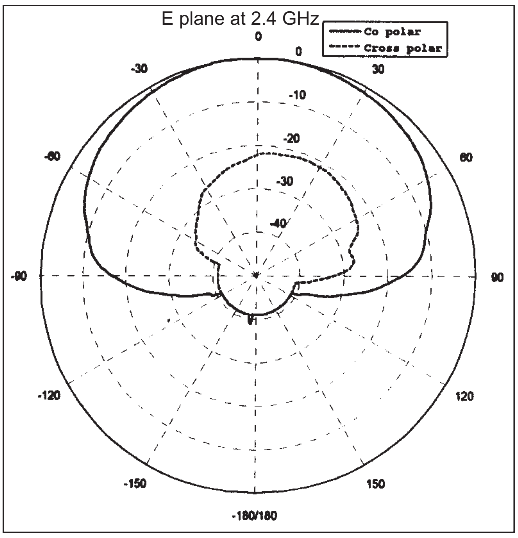

Figure 13(a) E plane polar radiation pattern for coaxial probe feed

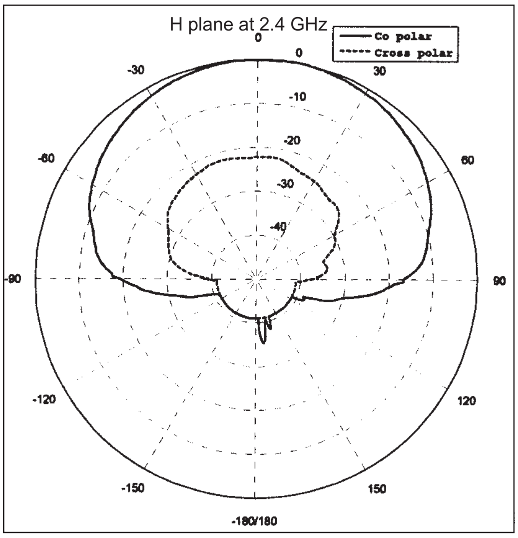

Figure 13(b) H plane polar radiation pattern for coaxial probe feed

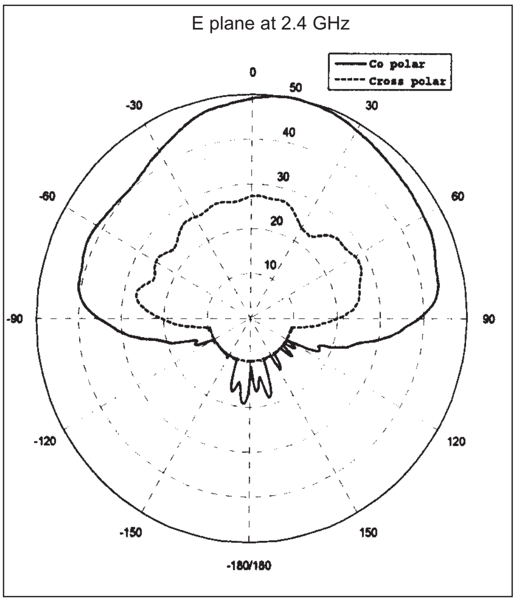

Figure 14(a) E plane polar radiation pattern for transmission line feed

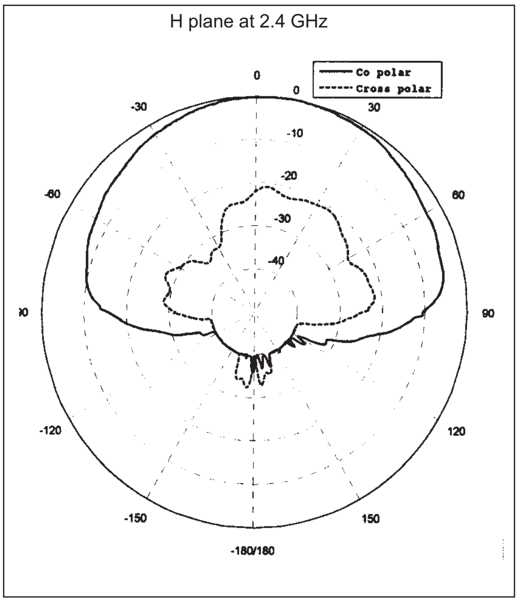

Figure 14(b) H plane polar radiation pattern for transmission line feed

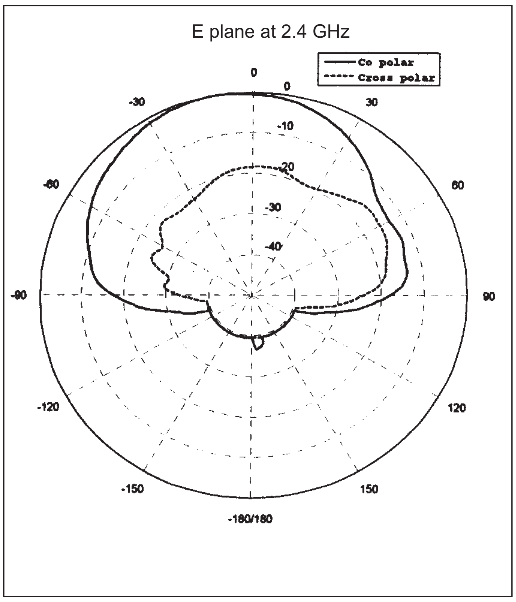

Figure 15(a) E plane polar radiation pattern for proximity coupled feed

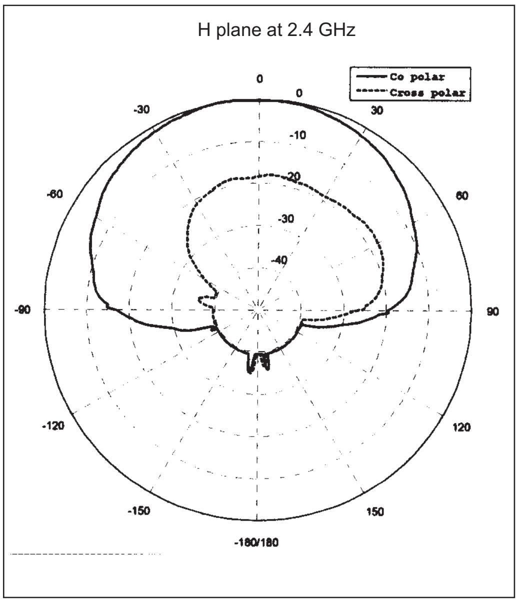

Figure 15(b) H plane polar radiation pattern for proximity coupled feed

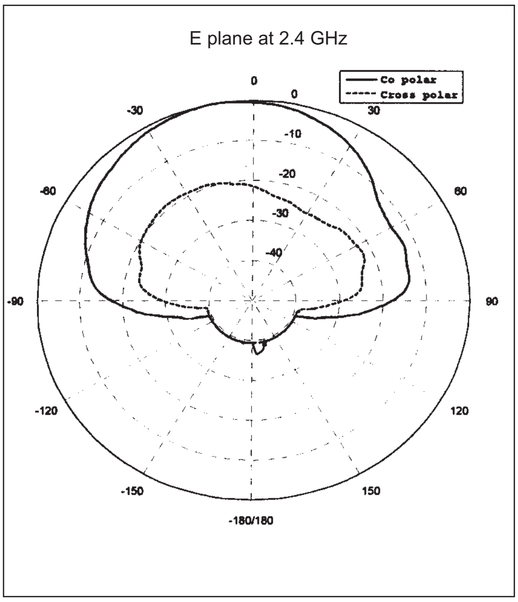

Figure 16(a) E plane polar radiation pattern for aperture coupled feed

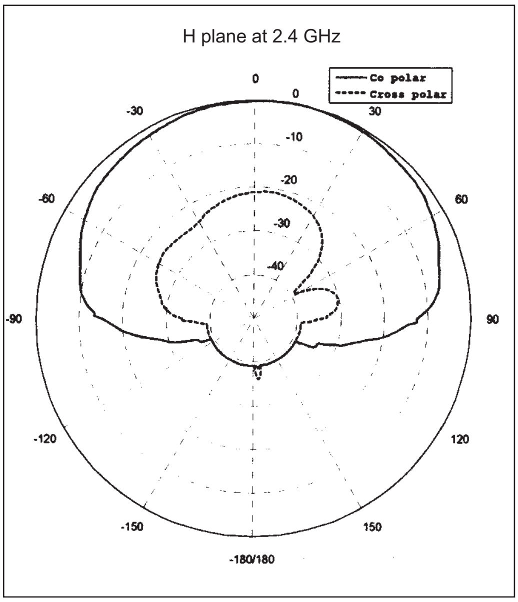

Figure 16(b) H plane polar radiation pattern for aperture coupled feed

Comparison of difference between the simulated and measured HPBW shows that the highest percentage is evident in TLF-MPA (about 8%). This is caused by the spurious radiation imminent along the length of the feed, thus reducing the power available for input to patch and affects matching. The two non-contacting feeds (ACF- and PCF-MPAs) showed less variance between simulated and measured HPBW, compared to direct contact feeds (TLF- and CPF-MPA). This can be proven by observing ACF-MPA's simulated H plane HPBW which differs the least from its measured result, while the least E plane HPBW difference between measured and simulated is also shown in another non-contacting feed, the PCF-MPA. The cause of this is; since power for non-contacting feeds is coupled to patch over layers from feed, this mechanism produces a radiation characteristic that is easily predicted through simulation, especially in MoM, while at the same time agreeing to a good impedance match.

In terms of gain and directivity, the simulated values of each antenna produced slightly larger value as compared to measured. This is a proof of slight losses when the antennas are operated in practice. The lowest measured gain among the four is produced by CPF-MPA, while non-contacting feeds show a higher gain level. This is directly related to the E plane HPBW characteristic, where a narrower E plane will produce a larger gain at a specific direction [12]. In this study, the CPF-MPA produced the largest E plane (HPBW of 96°) which is the main cause of its poor gain characteristics. In contrast, the highest gain is produced by ACF-MPA, which has the narrowest E plane HPBW.

The isolation levels produced by all feed are at an acceptable level, and ACF-MPA's E and H plane produced the lowest value of 20.96 dB. This is caused by the high cross polarization level, due to the same substrates used on both layers, whereas conventional ACF-MPA design uses higher ε_r at the top layer and a lower ε_r value at the bottom layer [8]. The highest isolation at both E and H plane is produced by PCF-MPA, due to its high h, moderate W and low cross polarization level [3, 12].

From the results, it is concluded that the gain is more influenced by the E plane isolation rather than the H plane isolation. The higher the isolation is, the better its gain and directivity values produced [8]. It is also shown in this analysis that the non-contacting feeding techniques have better efficiencies (e) which are in the magnitude of 98%, in producing its gain value from a given directivity. Direct contacting feeds suffers a higher level of losses, up to 88% to 90%.

5.0 CONCLUSIONS

A method of design, optimization, fabrication, measurement and result analysis is presented in comparing four most common feeding techniques to a microstrip patch antenna. The design and simulation has utilized the process equations and structural simulation tools. A circuit model for each type of feed and its parameter calculation equations is also adopted in this work. All antennas designed and measured are proven operable, with a sufficient amount of return loss, gain, and radiation characteristics in the 2.4 GHz ISM Band. Each method of the feeding techniques has their advantages and disadvantages as listed in the Table 5 and 6.

Table 5 The summary and comparison of the measured and simulated RL, fres and BW

Type of feed	Rep model	Return loss (dB)	Resonant freq (GHz)	Band width (%)	Res freq variation (%)	Band width variation (%)
Coaxial Probe Feed	MoM	–31.760	2.290	2.180	1.031	1.357
	Meas	–23.350	2.425	2.210		
Microstrip Line Feed	MoM	–22.480	2.360	2.540	0.415	18.503
	Meas	–30.770	2.410	2.070		
Aperture Coupled Feed	MoM	–25.530	2.350	3.820	2.991	1.799
	Meas	–24.090	2.474	3.890		
Proximity Coupled Feed	MoM	–31.934	2.320	3.840	1.639	6.341
	Meas	–21.360	2.440	4.100		

Table 6 The summary and comparison of the measured and simulated HPBW, Gain and Directivity

Parameters		CPF-MPA		TLF-MPA		ACF-MPA		PCF-MPA	
		E-Plane	**H-Plane**	**E-Plane**	**H-Plane**	**E-Plane**	**H-Plane**	**E-Plane**	**H-Plane**
Max co-polarization (-dBm)		–8.93	–8.91	–9.59	–10.32	–10.55	–10.83	–10.15	–10.52
Max cross-polarization (-dBm)		–30.10	–30.75	–31.56	–31.08	–29.43	–31.68	–36.14	–38.17
Isolation at 0° (dB)		21.18	21.84	21.99	20.76	20.96	20.96	25.99	27.64
HPBW (°)	Sim	101.5	110.2	102.5	100.6	84.7	110.6	89.7	101.9
	Meas	96.0	106.0	94.0	92.0	81.0	107.0	86.0	98.0
Directivity (dB)	Sim	7.0699		7.2092		7.9518		8.0387	
	Meas	7.0150		7.1470		7.8430		7.8860	
Gain (dB)	Sim	6.2605		6.5177		7.9146		7.8358	
	Meas	6.064		6.2130		7.6930		7.5910	

REFERENCES

[1] Godara, L. C. 2002. *Handbook of Antennas in Wireless Communication*. Florida: CRC Press LLC.

[2] Vajha, S. and S. N. Prasad. 2000. Design and Modeling of a Proximity Coupled Patch Antenna. *Conference on Antennas and Propagation for Wireless Communications*. 6-8 Nov. Massachusetts IEEE-APS: 43-46.

[3] Garg, R., P. Bhartia, I. Bahl, and A. Ittipiboon. 2001. *Microstrip Antenna Design Handbook*. London: Artech House.

[4] James, J. R. and P. S. Hall. 1989. *Handbook of Microstrip Antennas*, London: Peter Peregrinus Ltd.

[5] Kapsidis, D., M. T. Chryssomallis, and C. G. Christodoulou. 2003. An Accurate Circuit Model of a Microstrip Patch Antenna for CAD Applications. *Antennas and Propagation Society International Symposium*. 22-27 June. Greece IEEE: 120-123.

[6] Balanis, C. A. 1997. *Antenna Theory: Analysis and Design*. 2nd Ed. New York: John Wiley and Sons.

[7] Soh, P. J., M. K. A. Rahim, A. Asrokin, M. Z. A. Abdul Aziz. 2005. Modeling of Different Feeding Techniques for a Microstrip Patch Antenna. *MMU International Symposium on Information and Communications Technologies (M2USIC'05)*, Proceedings of the. Nov 24th-25th. Malaysia: Malaysia Multimedia University (MMU), TS05: 9-13.

[8] Soh, P. J., M. K. A. Rahim, A. Asrokin. 2006. Design, Modeling and Comparison of Non-Contacting Feeds for a Microstrip Patch Antenna, *IEEE International Conference on Computer & Communication Engineering (ICCCE 06)*. May 9th-11th. Malaysia IEEE Malaysia Chapter.

[9] Asrokin, A., M. K. A. Rahim, P. J. Soh. 2006. Slotted Square Microstrip Antenna Using the Proximity Feeding Technique for Dual Band Application, *IEEE International Conference on Computer & Communication Engineering (ICCCE 06)*. May 9th-11th. Malaysia IEEE Malaysia Chapter.

[10] Kyriacou, G. A., A. A. Mavrides, A. O. Breinbjerg, and J. N. Sahalos. 2000. A Design Procedure for Aperture-coupled Microstrip Antennas Based on Equivalent Network. *AP2000 Millennium Conference on Antennas & Propagation*, Proceedings of. April. Davos, Switzerland.

[11] Soh, P. J., M. K. A. Rahim, A. Asrokin, M. Z. A. Abdul Aziz. 2005. Comparative Studies on Performance of Different Feeding Techniques Using Circuit Model for a Microstrip Patch Antenna. *IEEE Asia Pacific Conference on Applied Electromagnetics (APACE'05)*, Proceedings of the. Dec 20th-21st. Malaysia IEEE AP/MTT/EMC Joint Chapter.

[12] Soh, P. J. 2005. Microstrip Antenna with Different Feeding Techniques, Universiti Teknologi Malaysia: M. Eng. Thesis.

[13] Rahim, M. K. A. 2003. Wideband Active Antenna, University of Birmingham Ph.D. Thesis.